THE JOURNAL OF BIOLOGICAL CHEMISTRY
Vol. 277, No. 7, Issue of February 15, pp. 5426–5432, 2002

Printed in U.S.A.

Formation of Functional Heterodimers between the TASK-1 and TASK-3 Two-pore Domain Potassium Channel Subunits*

Received for publication, July 27, 2001, and in revised form, November 20, 2001
Published, JBC Papers in Press, December 3, 2001, DOI 10.1074/jbc.M107138200

Gábor Czirják and Péter Enyedi‡

From the Department of Physiology, Semmelweis University, H-1444 Budapest, Hungary

The potassium channels in the two-pore domain family are widely expressed and regulate the excitability of neurons and other excitable cells. These channels have been shown to function as dimers, but heteromerization between the various channel subunits has not yet been reported. Here we demonstrate that two members of the TASK subfamily of potassium channels, TASK-1 and TASK-3, can form functional heterodimers when expressed in *Xenopus laevis* oocytes. To recognize the two TASK channel types, we took advantage of the higher sensitivity of TASK-1 over TASK-3 to physiological pH changes and the discriminating sensitivity of TASK-3 to the cationic dye ruthenium red. These features were clearly observed when the channels were expressed individually. However, when TASK-1 and TASK-3 were expressed together, the resulting current showed intermediate pH sensitivity and ruthenium red insensitivity (characteristic of TASK-1), indicating the formation of TASK-1/TASK-3 heterodimers. Expression of a tandem construct in which TASK-3 and TASK-1 were linked together yielded currents with features very similar to those observed when coexpressing the two channels. The tandem construct also responded to AT_{1a} angiotensin II receptor stimulation with an inhibition that was weaker than the inhibition of homodimeric TASK-1 and greater than that shown by TASK-3. Expression of epitope-tagged channels in mammalian cells showed their primary presence in the plasma membrane consistent with their function in this location. Heteromerization of two-pore domain potassium channels may provide a greater functional diversity and additional means by which they can be regulated in their native tissues.

Potassium channels play a pivotal role in adjusting the excitability of neurons and endocrine cells by controlling the resting membrane potential. Two large families of K^+ channels have been identified so far that can drive the resting membrane potential (E_m) toward hyperpolarization. Inwardly rectifying potassium channels conduct considerable currents around the K^+ equilibrium potential, but their outward current diminishes upon depolarization. Therefore, these channels stabilize the resting E_m without markedly influencing depolarizing membrane potential changes. In contrast, members of the two-pore domain (2P)[1] potassium channels provide substantial currents not only at the resting E_m but also in the depolarized state. Moreover, the repolarizing current of 2P potassium channels is maintained at a given potential, because they activate instantaneously and, with the exception of TWIK-2 (1), they do not inactivate. Therefore, in addition to controlling the resting E_m, 2P potassium channels are also involved in the regulation of action potential duration and firing patterns in neurons (2, 3) as well as in the control of membrane potential changes in stimulated endocrine (4) and chemoreceptor (5) cells (see Refs. 6 and 7 for review).

Two-pore domain K^+ channels are classified as a family based on their similar molecular architecture. Each subunit contains four transmembrane segments and two pore-forming domains: one located between the first and second transmembrane segments and another between the third and fourth transmembrane segments. This topology assumes that both the N and C termini of the subunits are intracellular. The selectivity filter of K^+ channels being made up of four pore domains is the reason for the requirement to form dimers. In addition to these theoretical considerations, dimer formation of 2P channel subunits has been also demonstrated experimentally (8–10). The cloned mammalian 2P channels have been classified into five subfamilies based on their primary sequences and electrophysiological and regulatory properties. The TWIK (tandem of pore domains in a weakly inwardly rectifying K^+ channel) subfamily contains TWIK-1 (11), TWIK-2 (1), and KCNK7 (12) (although the latter channel could not be expressed functionally). TWIKs are regulated by protein kinase C and by changes in intracellular pH. Members of the TREK (TWIK-related K^+ channel) subfamily TREK-1 (13), TREK-2 (14, 15), and TRAAK (16) are mechanosensitive channels activated by unsaturated fatty acids. Of the THIK (tandem pore domain halothane-inhibited K^+ channel) subfamily members, THIK-1 (17) can also be activated by arachidonic acid, whereas THIK-2 failed to display channel behavior upon heterologous expression, despite its targeting to the plasma membrane (17). The further subfamilies are interrelated by their strong pH sensitivity. TASK-2 (18), TALK-1 (19), and TALK-2 (19) (also termed as TASK-4 (20)) are activated by extracellular (EC) alkaline pH, whereas two other TASK (TWIK-related acid-sensitive K^+) channels, TASK-1 (21–23) and TASK-3 (24), are classified to another subfamily despite sharing the name with TASK-2 and TASK-4. Both TASK-1 and TASK-3 are inhibited by EC acidification, an effect mediated by histidine 98 of TASK-3 (25), which is also conserved in TASK-1 (but not in TASK-2 or TASK-4). Recent studies indicated that stimulation of certain

* This work was supported by Hungarian National Research Fund Grant OTKA 032159 and Hungarian Medical Research Council Grant ETT-248/2000. The costs of publication of this article were defrayed in part by the payment of page charges. This article must therefore be hereby marked "*advertisement*" in accordance with 18 U.S.C. Section 1734 solely to indicate this fact.

‡ To whom correspondence should be addressed: Dept. of Physiology, Semmelweis University, P.O. Box 259, H-1444 Budapest, Hungary. Tel.: 36-1-266-2755, Ext. 4079; Fax: 36-1-266-6504; E-mail: enyedi@puskin.sote.hu.

[1] The abbreviations used are: 2P, two-pore domain; EC, extracellular; MES, 4-morpholineethanesulfonic acid; HA, hemagglutinin; FBS, fetal bovine serum; PBS, phosphate-buffered saline; RR, ruthenium red.

G protein-coupled receptors inhibits TASK-1 channels (2–4); this effect is mediated by phospholipase C activation (26).

In all of the above-mentioned studies, 2P channels were expressed as homodimers (for review see Ref. 27). Recently, it was also demonstrated that both the P_1 and the P_2 domains of KCNK3 (TASK-1) contribute to the pore within the homodimer (10). The possible heterodimer formation between THIK-1 and THIK-2 (17) and KCNK6 and KCNK7 (12) has been studied in detail. However, these studies concluded that neither THIKs nor these KCNKs can form heterodimers, because the THIK-1 current was not influenced by overexpression of the nonfunctional THIK-2, and coexpression of KCNK6 and KCNK7 did not yield a functional K^+ channel (2). In the present report we demonstrate for the first time that two members of the TASK subfamily, TASK-1 and TASK-3, are capable of constituting functional heterodimers when expressed in *Xenopus laevis* oocytes. The pharmacological and regulatory properties of the TASK-1/TASK-3 heterodimer is clearly different from those of each of the homodimers, adding to the diversity of potassium channels that affect the function of excitable cells.

EXPERIMENTAL PROCEDURES

Materials—Enzymes and kits of molecular biology applications were purchased from Ambion (Austin, TX), Amersham Biosciences, Inc., Fermentas (Vilnius, Lithuania), New England Biolabs (Beverly, MA), and Promega (Madison, WI). All other chemicals of analytical grade were obtained from Fluka (Buchs, Switzerland), Promega, and Sigma.

Cloning of TASK-3 cDNA and Construction of Tandem TASK-3/TASK-1 Channels—The coding region of TASK-3 was amplified from total RNA prepared from rat adrenal zona glomerulosa using *Pfu* turbo DNA polymerase after reverse transcription. PCR primers were designed on the basis of the published rat TASK-3 sequence. The forward primer was 5′-ggcatATGAAGCGGCAGAATGTGCG-3′ (T3-s), and the reverse primer (T3end-a) was 5′-cctctctagACTTAGATGGACTTGCGACG-3′. The additional bases at the 5′ ends (indicated by lowercase letters) introduced *Nde*I and *Xba*I restriction sites to the forward and reverse primers, respectively. The PCR product was digested with *Xba*I and cloned into the *Xba*I-*Eco*RV-digested Bluescript pKS phagemid (Stratagene). This construct was then subcloned into the pEXO vector containing the 5′- and 3′-untranslated regions of the *Xenopus* globin gene. The sequence of the construct (pEXO-TASK-3) was determined from both directions by automated sequencing.

Partially overlapping sense (T(3+1)LIGs: 5′-GTCCATCAAGCGGCAGAACGTGCGC-3′) and antisense (T(3+1)LIGa: 5′-CTGCCGCTTGATGGACTTGCGACGGATG-3′) oligonucleotides were designed for linking the coding sequences of TASK-3 and TASK-1. The sequence of the oligonucleotides covered the C-terminal end of the TASK-3 and the N-terminal beginning of the TASK-1 coding sequences in frame. PCR products were amplified (15 cycles) from pEXO-TASK-3 with the sense T3forw (corresponding to bases 268–290 of TASK-3) and the antisense T(3+1)LIGa primers. PCR was also performed from pEXO-TASK-1 with the sense T(3+1)LIGs and the antisense T1rev (corresponding to bases 611–631 of TASK-1). The two PCR products were then mixed, allowed to hybridize by their overlapping T(3+1)LIGs and T(3+1)LIGa primer regions, and elongated without primers. This was followed by further amplification (15 cycles) in the presence of T3forw and T1rev primers. The resulting T3forw-T1rev product was digested with *Kpn*2I (which cuts within the TASK-3 half of the sequence) and was ligated into the *Kpn*2I-*Sma*I digested pEXO-TASK-3. (*Sma*I creates a blunt end at the multiple cloning site of pEXO at the 3′ end of the TASK-3 insert). To add the missing piece of TASK-1 to this construct, the *Nco*I-*Bam*HI fragment of the resulting clone was replaced with the *Nco*I-*Bam*HI fragment of pEXO-TASK-1. (The *Nco*I site is within the TASK-1 part of the T3forw-T1rev amplification product, and *Bam*HI is in the pEXO cloning site downstream of the *Sma*I site.) The region of the two channels originating from the PCR amplification was verified by sequencing. The pEXO-TASK-(3+1) construct coded for a polypeptide chain, in which the last amino acid residue (Ile) of TASK-3 is followed by the second residue of TASK-1 (Lys).

cRNA Synthesis—TASK-1, TASK-3, TASK-(3+1), TRAAK, TREK-1 and the angiotensin II (AT_{1a}) receptor cRNA were synthesized *in vitro* according to the manufacturer's instructions (Ambion mMESSAGE mMACHINE™ T7 *in vitro* transcription kit) using the *Xba*I linearized pEXO-TASK-1 (21), pEXO-TASK-3, pEXO-TASK-(3+1), pEXO-TRAAK (28), and pEXO-TREK-1 (13) constructs and the *Not*I linearized plasmid, comprising the coding sequence and 5′-untranslated region of rat AT_{1a} angiotensin II receptor (kindly provided by Dr. K. E. Bernstein).

Animals and Tissue Preparation and X. laevis Oocyte Injection—Mature female *X. laevis* frogs were obtained from Amrep Reptielen (Breda, Netherlands). The frogs were anesthetized by immersion into benzocaine solution (0.03%). Ovarian lobes were removed, and the tissue was dissected and treated with collagenase (1.45 mg/ml, 148 units/mg, type I; Worthington Biochemical Corp., Freehold, NJ) and continuous mechanical agitation in Ca^{2+}-free OR2 solution containing 82,5 mM NaCl, 2 mM KCl, 1 mM $MgCl_2$, 5 mM HEPES, pH 7.5, for 1.5–2 h. Stage V and VI oocytes were defolliculated manually and kept at 18 °C in modified Barth's saline containing 88 mM NaCl, 1 mM KCl, 2.4 mM $NaHCO_3$, 0.82 mM $MgSO_4$, 0.33 mM $Ca(NO_3)_2$, 0.41 mM $CaCl_2$, 20 mM HEPES buffered to pH 7.5 with NaOH and supplemented with penicillin (100 units/ml), streptomycin (100 μg/ml), sodium pyruvate (4.5 mM), and theophyllin (0.5 mM). The oocytes were injected 1 day after defolliculation. Fifty nanoliters of the appropriate RNA solution was delivered with Nanoliter Injector (World Precision Instruments, Saratosa, FL). Electrophysiological experiments were performed 3 or 4 days after the injection.

Electrophysiology—Membrane currents were recorded by two-electrode voltage clamp (OC-725-C; Warner Instrument Corp., Hamden, CT) using microelectrodes made of borosilicate glass (Clark Electromedical Instruments, Pangbourne, UK) with a resistance of 0.3–1 MΩ when filled with 3 M KCl. The currents were filtered at 1 kHz, digitally sampled at 1–2.5 kHz with a Digidata Interface (Axon Instruments, Foster City, CA), and stored on a PC/AT computer. Recording and data analysis were performed using pCLAMP software 6.0.4 (Axon Instruments). The experiments were carried out at room temperature, and the solutions were applied by a gravity-driven perfusion system. Low $[K^+]$ solution contained 95.4 mM NaCl, 2 mM KCl, 1.8 mM $CaCl_2$, 5 mM HEPES. High $[K^+]$ solution contained 80 mM K^+ (78 mM Na^+ of the low $[K^+]$ solution was replaced with K^+). Unless otherwise stated, the pH of every solution was adjusted to 7.5 with NaOH. Perifusing solutions with a pH of <6.5 were buffered by including 5 mM MES. Background K^+ currents were measured in high EC $[K^+]$ at the end of 300-ms-long voltage steps to −100 mV applied in every 3 s. The holding potential was 0 mV. Where possible, the inward current in high $[K^+]$ was corrected for the small nonspecific leak measured in 2 mM EC $[K^+]$.

Transfection and Immunocytochemistry of Epitope-tagged TASK-1 and TASK-3 Channels—Oligonucleotide dimers coding for the *myc* (residues 410–419 of human c-*myc*, EQKLISEEDL) and HA (residues 99–107 of human influenza virus hemagglutinin, YPYDVPDYA) epitopes were ligated in the unique *Nru*I and *Kpn*2I restriction enzyme sites of pEXO-TASK-1 and pEXO-TASK-3, respectively. Hybridization of the sense *myc* oligonucleotide (5′-GAGGAGCAGAAGCTGATCTCAGAGGAGGACCTG-3′) with its reverse complement created blunt ends, whereas the sense (5′-CCGGGCTACCCTTACGACGTCCCTGACTACGCC-3′) and antisense (5′-CCGGGGCGTAGTCAGGGACGTCGTAAGGGTAGC-3′) HA oligonucleotides were designed to form overhanging *Kpn*2I-compatible ends in the appropriate reading frame. Correct insertion of the epitope coding regions was checked by sequencing. The epitope-tagged coding sequences were subcloned also into pcDNA3.1+ (Invitrogen) for expression in mammalian cells.

For immunocytochemistry HEK cells were grown on glass coverslips in Dulbecco's modified Eagle's medium supplemented with 10% FBS and were transfected for 6 h with TASK-1-HA-pcDNA3 or TASK-3-HA-pcDNA3 constructs (1 μg) in 1.2 ml of Opti-MEM containing 2 μl of LipofectAMINE. Two days after the transfection the cells were fixed in 2% (w/v) paraformaldehyde in PBS for 10 min and washed three times with PBS containing 10% (v/v) fetal bovine serum (PBS-FBS). The cells were then incubated for 1 h with monoclonal anti-HA epitope antibody (Covance PRB 150C, 1:1000 dilution) in the presence of 0.2% saponin in PBS-FBS, followed by three 5-min washes before incubation for 1 h with Alexa Fluor-488 goat anti-mouse IgG for TASK-1 and with Alexa Fluor-594 goat anti-mouse IgG (Molecular Probes) for TASK-3 (each at 1:1000 dilution). For simultaneous detection of TASK-1 and TASK-3, the cells were cotransfected with TASK-1-myc-pcDNA3 and TASK-3-HA-pcDNA3 constructs (1 μg each, as above). During the immunostaining procedure and the incubation with the anti-HA epitope antibody and with the secondary Alexa Fluor 594 anti-mouse antibody (as above), the cells were washed and stained with a monoclonal fluorescein isothiocyanate-conjugated anti-*myc* antibody (Covance FITC-150L, 1:50 dilution). After three final washes (each for 5 min in PBS-FBS), the coverslips were mounted for confocal microscopy. The cells were examined by an inverted Zeiss 410 laser confocal microscope with a (100×) oil immersion lens.

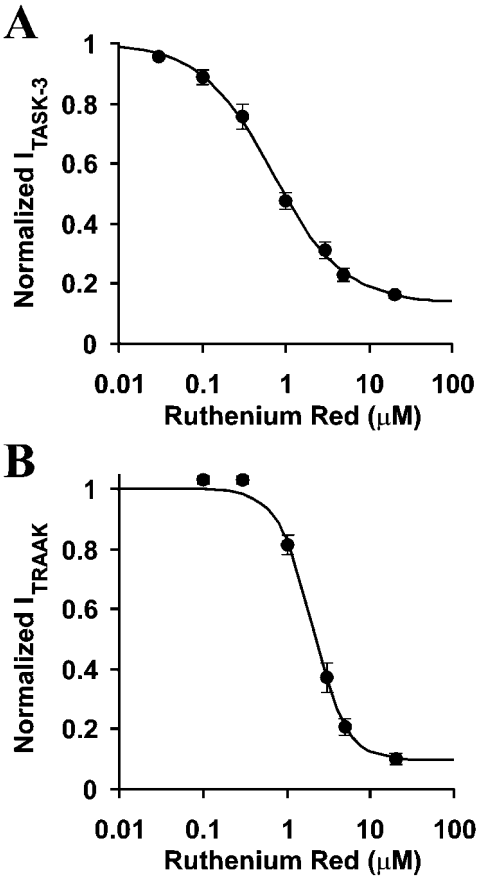

FIG. 1. **Ruthenium red inhibits TASK-3 and TRAAK.** Oocytes expressing TASK-3 (*A*, $n = 7$) or TRAAK (*B*, $n = 5$) were treated with different concentrations (0.03, 0.1, 0.3, 1, 3, 5, and 20 μM) of ruthenium red. The currents were measured at −100 mV in high (80 mM) EC [K^+], corrected for the small nonspecific leak in 2 mM EC [K^+] and normalized to the control value (without RR). The *smooth curves* of incomplete inhibition were fitted according to a modified Hill equation.

Statistics and Calculations—The data are expressed as the means ± S.E. Normalized dose-response curves were fitted (least squares method; Sigmaplot, Jandel Corporation) to the following Hill equation: $y = 1/(1 + (c/K_{½})^n)$, where c is the concentration, $K_{½}$ is the concentration at which half-maximal inhibition occurs, and n is the Hill coefficient. Where the treatment failed to cause complete inhibition, a modified form of the equation was used: $y = \varphi/(1 + (c/K_{½})^n) + (1 - \varphi)$, where φ is the fraction maximally inhibited by the treatment.

RESULTS

Characterization of Individually Expressed TASK and TREK Channels—In a recent study we found that TASK-1 and TASK-3 channels can be distinguished by their different sensitivity to the polycationic compound, ruthenium red (RR).[2] With the aim of applying RR as a potential tool discriminating between different members of the 2P domain potassium channel family, we analyzed the inhibitory effect of RR on TASK-1, on TASK-3, and also on TRAAK and TREK-1 channels in more detail. The current was monitored at −100 mV in the presence of 80 mM extracellular [K^+], a condition that gives a large signal of the expressed channels with only minor contamination by other endogenous currents of the oocytes (4).

As shown in Fig. 1, TASK-3 and TRAAK currents were greatly reduced by RR with a half-maximal inhibitory concentration of 0.7 and 2 μM, respectively. Interestingly, the inhibition of TRAAK followed a much steeper dose-response relationship than the inhibition of TASK-3. This was also reflected in the Hill coefficients calculated for the inhibitory curves. The Hill coefficient for TASK-3 channels was found to be 1.0, indicating the binding of one RR molecule to one functional channel (dimer). In contrast, TRAAK inhibition by RR showed a Hill coefficient of 2.1, suggesting multiple RR-binding sites. The inhibitory effect of RR on both channels was found to be voltage-independent (Fig. 2), indicating that the RR-binding sites on TASK-3 and TRAAK lay outside the transmembrane electrical field; accordingly a direct interference of the inhibitor with the pore of the channel is very unlikely. The rapid onset of the inhibition (not shown) suggests that RR acts from the extracellular side of the channels.

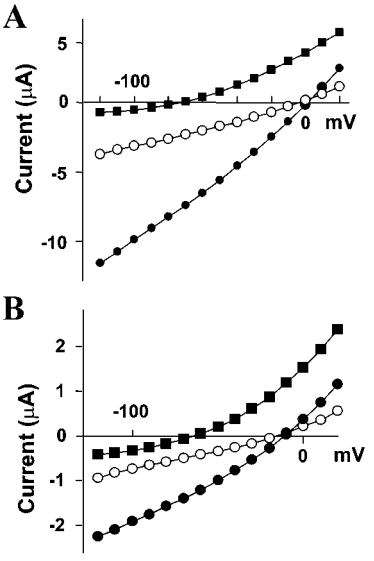

FIG. 2. **TASK-3 and TRAAK inhibition by ruthenium red is not voltage-dependent.** Current-voltage relationships of an oocyte expressing TASK-3 (*A*) or TRAAK (*B*) were plotted in 2 mM EC [K^+] (■) and in 80 mM EC [K^+] without (●) or with 3 μM ruthenium red (○). The currents were recorded at the end of 300-ms voltage steps from −120 mV to +20 mV in 10-mV increments from a holding potential of 0 mV.

In contrast to the prominent inhibition of TASK-3 and TRAAK channels by RR, their close relatives, TASK-1 and TREK-1, respectively, were not inhibited by RR even at micromolar concentration (4.5 ± 1.2% inhibition of TASK-1 by 5 μM RR ($n = 14$) and less than 10% inhibition of TREK-1 by 20 μM ($n = 5$)). Based on these results, RR has been identified as an excellent tool to differentiate between the individual members within both the TASK and TREK family of potassium channels.

As reported earlier, an additional feature discriminating between TASK-1 and TASK-3 channels is their sensitivity to extracellular acidification, TASK-1 (on the contrary to TASK-3) being highly sensitive to pH changes between 7.5 and 6.5 (21, 22, 24).[2]

Coexpression of TASK-1 and TRAAK Yields Currents with Features That Are Consistent with Linear Combination of TASK-1 and TRAAK Homodimers and Do Not Indicate Heterodimer Formation—First, we investigated the behavior of TASK-1 and TRAAK channels expressed simultaneously in *Xenopus* oocytes in different ratios. Given the differential pH and ruthenium red sensitivities of the channels, their characteristics could be best evaluated when the degrees of inhibition by acidification (a pH step from 7.5 to 6.5) and RR (5 μM) were plotted one against the other (Fig. 3). The positions of the two populations of homodimers (when only one form of the channels is expressed) is clearly separated in the extreme ends of the plot. TASK-1 homodimers that are insensitive to RR but highly sensitive to pH changes appear in the *lower right*, whereas TRAAK homodimers that are practically insensitive to acidifi-

[2] G. Czirják and P. Enyedi, (2002) *Mol. Endocrinol.*, in press

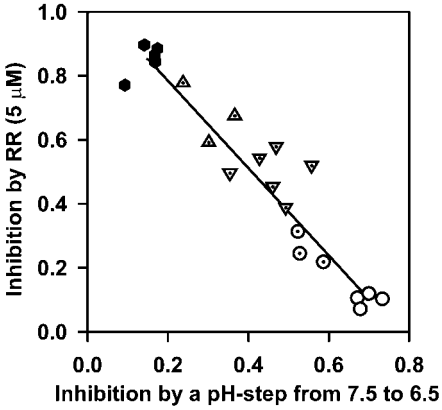

FIG. 3. **Ruthenium red and pH sensitivity of the current of oocytes coexpressing TASK-1 and TRAAK in different ratios.** The injected amounts of cRNAs were adjusted to give about equal current amplitudes in oocytes expressing only TASK-1 (*open circle*) or TRAAK (*filled hexagon*). Other oocytes received the mixtures of these TASK-1 and TRAAK cRNA solutions in different ratios: 3:1 (*circle* with *dot*), 1:1 (*inverted triangle* with *dot*), and 1:3 (*triangle* with *dot*), respectively. Ruthenium red and pH sensitivity was estimated by applying a pH step to 6.5 from 7.5, followed by challenging the same oocyte with 5 μM RR (at pH 7.5). The *straight line* connects the averages of the pure TASK-1 and TRAAK data points.

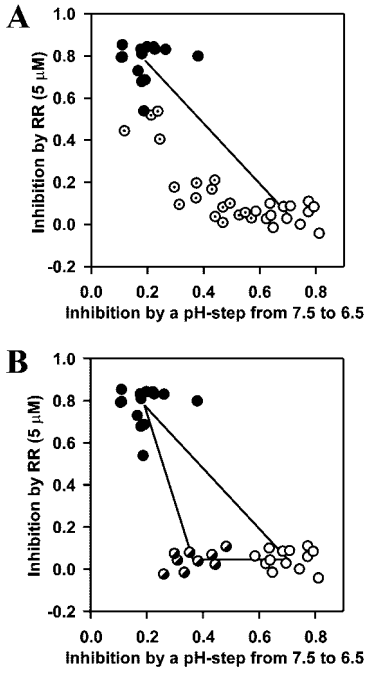

FIG. 4. **RR and pH sensitivity of oocytes expressing TASK-1, TASK-3, TASK-1 and TASK-3, or the TASK-3/TASK-1 tandem channel.** *A*, in oocytes expressing only TASK-1 (○), expressing only TASK-3 (●), or coexpressing TASK-1 and TASK-3 in different ratios (⊙), the ruthenium red and pH inhibition was measured as described in detail in the legend to Fig. 3. The *straight line* connects the averages of the pure TASK-1 and TASK-3 points. *B*, ruthenium red and pH dependence of the K^+ current in oocytes expressing the TASK-3/TASK-1 tandem channel (◑). The same TASK-1 and TASK-3 points as in *panel A* are also plotted. The angles of the represented triangle are formed by the averages of the data points of the three distinct channel types.

cation but are strongly inhibited by RR in the *upper left area* of the *graph*. When the characteristics of the coexpressed channels was plotted in the same graph, their data points all fell on the *straight line* connecting the clear TASK-1 and TRAAK populations (Fig. 3). Depending on the ratios of the two channels, the points fell closer or farther from the respective ends representing the homodimers. Such distribution of channel behavior is expected if various amounts of the two kind of homodimer channels operate independently, and therefore these data did not indicate that TASK-1 and TRAAK channels would form heterodimers.

Coexpression of TASK-1 and TASK-3 Yields Currents with Features That Are Distinct from Linear Combination of TASK-1 and TASK-3 Homodimer Channel Currents—Clearly different results were obtained when TASK-1 and TASK-3 channels were coexpressed in the oocytes. TASK-1 or TASK-3 channels expressed alone are also presented with two, clearly distinguishable set of data points. The 70.4 ± 1.9 and 4.5 ± 1.2% (n = 14) inhibition of TASK-1 by acidification and RR, respectively, contrasted with the 19.3 ± 1.9 and 77.6 ± 2.3% (n = 14) inhibition by the same manipulations of TASK-3 channels. However, after coexpressions of the two channels, all the data points fell under the line connecting the TASK-1 and TASK-3 values (Fig. 4*A*). This result cannot be explained by formation of various proportions of simple homodimers and indicates the presence of significant amounts of heterodimer channels with new inhibitor sensitivity profiles.

The TASK-(3+1) Tandem Channel Has Intermediate pH and Low RR Sensitivity—It is difficult to deduce the true characteristics of the heterodimer channels in terms of their pH and RR sensitivities in the above experiments because of the simultaneous presence of homodimers. To overcome this difficulty, we created a tandem version of TASK-3 and TASK-1 channels by joining the coding regions of the two channels to form one continuous protein. In this construct the C terminus of TASK-3 was fused to the N terminus of TASK-1. Such a tandem construct was expected to highly favor the assembly of the channels as heterodimers. Expressing the tandem channel in the oocytes induced large currents (13.3 ± 2.5 μA, n = 17), comparable in amplitude to the currents of TASK-1 and TASK-3. However, the pH and RR sensitivity values of the tandem channel was clearly distinct from both parent channels. It showed significant inhibition (36.4 ± 2.5%, n = 9) in response to a pH step form 7.5 to 6.5 (an intermediate pH sensitivity between TASK-1 and TASK-3 channels) and minimal inhibition (4.5 ± 1.5%, n = 9) by 5 μM RR (a feature of TASK-1 channels) (Fig. 4*B*). Remarkably, the data set given by the tandem channel showed an overlapping distribution with those obtained in the coexpression experiments confirming the formation of heterodimers in the latter (Fig. 4*A*).

The pH sensitivity of the tandem channel was compared with that of TASK-1 and TASK-3 homodimers in a wider pH range (Fig. 5). The intermediate pH sensitivity of the tandem channel between TASK-1 and TASK-3 was displayed at all tested values. Mild acidification, which inhibited TASK-1 but not TASK-3, was sufficient to cause a detectable decrease in the current of the tandem channel; however, the inhibition became complete only at a more acidic pH, which is characteristic for TASK-3. Consequently, the heterodimer is regulated in a wider pH range than either of the parent homodimers (Fig. 5).

The TASK-(3+1) Tandem Channel Is Inhibited by AT_{1a} Angiotensin II Receptor—TASK-1 has been shown to be inhibited by various calcium mobilizing agonists in heterologous expression systems (3, 4). Here we examined the inhibition of TASK-1, TASK-3, and the TASK-(3+1) tandem channel by the Ca^{2+}-mobilizing hormone angiotensin II in *Xenopus* oocytes expressing the channels and the AT_{1a} receptor. As shown in Fig. 6, angiotensin II (10 nM) inhibited TASK-1 channels significantly more potently than TASK-3 channels. The tandem channel again showed an intermediate inhibitory profile that was closer to that of TASK-1 than of TASK-3.

Localization of Epitope-tagged TASK-1 and TASK-3 Channels in Mammalian Cells—Although these studies in *Xenopus* oocytes clearly suggested that mammalian TASK-1 and

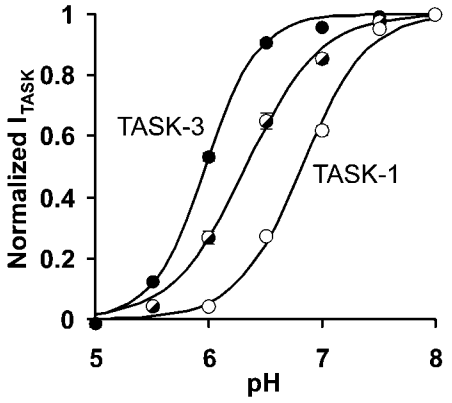

FIG. 5. **pH dependence of TASK-1, TASK-3, and the tandem channel.** Currents of oocytes expressing TASK-1 (○), TASK-3 (●), and the TASK-3/TASK-1 tandem channel (◑) were measured at different pH values in high (80 mM) extracellular $[K^+]$ at −100 mV. The currents were corrected for the small nonspecific leak in 2 mM EC $[K^+]$ at −100 mV and normalized to the maximum at pH 8. Each point represents the average of the normalized currents of 5 or 6 oocytes. In most cases the *error bars* are smaller than the *symbols*. The *smooth curves* were fitted according to Hill equations. (TASK-1 and TASK-3 pH dependence data are also published elsewhere.)

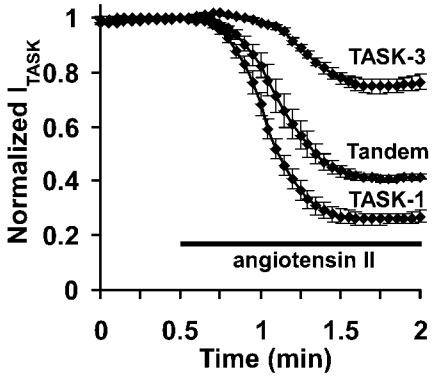

FIG. 6. **Inhibition of TASK-1, TASK-3 and the tandem channel by angiotensin II.** Currents of oocytes coexpressing AT1a angiotensin II receptor and TASK-1 or TASK-3 or the TASK-3/TASK-1 tandem were measured during angiotensin II (10 nM) stimulation (as indicated by the *bar*) in high (80 mM) extracellular $[K^+]$ at −100 mV. The currents were normalized to the value at the beginning of the stimulation. The *curves* are the averages of 10, 5, and 6 oocytes expressing TASK-1, TASK-3, and tandem, respectively.

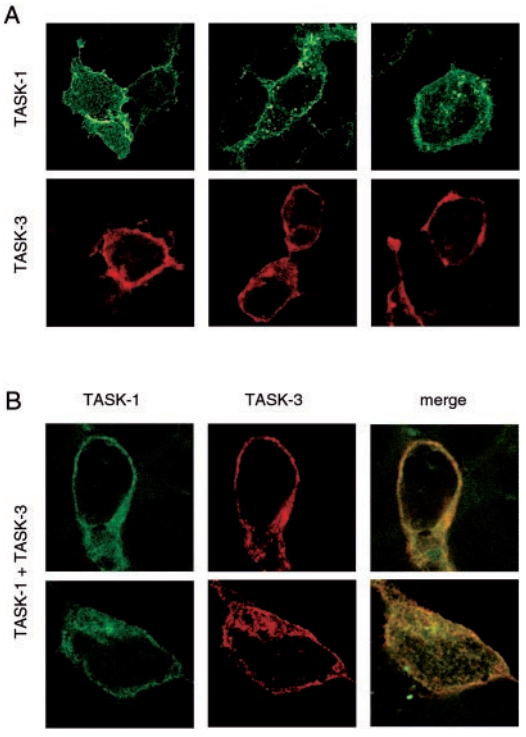

FIG. 7. **Localization of expressed TASK-1 and TASK-3 channels in HEK 293 cells.** Confocal images of HEK 293 cells expressing HA epitope-tagged TASK-1 or TASK-3 channels (*A*). Immunostaining with the primary HA-antibody was followed by incubation with a second antibody either conjugated to Alexa-488 (*green* for TASK-1) or to Alexa-594 (*red* for TASK-3). *B* shows images of cells coexpressing a *myc*-tagged TASK-1 and HA-tagged TASK-3 immunostained with both anti-HA (*red*) and anti-myc (*green*) antibodies as detailed under "Experimental Procedures." The cells were examined by confocal microscopy using the 488 and 568 laser lines for detection of green and red fluorescence, respectively.

TASK-3 channels can form heterodimers, we wanted to determine whether the two channels show similar localization in mammalian cells. For this purpose the two channels were tagged with HA and *myc* epitopes. The epitope tags were inserted into the intracellular tail, where they were expected not to interfere with the N-terminal leading sequence or the C-terminal putative PDZ-binding domain (in TASK-1). The tagged channels were also tested in oocytes and found completely functional. Immunocytochemical analysis of TASK-1 and TASK-3 channels expressed in HEK-293 cells (Fig. 7) and NIH 3T3 cells (not shown) revealed the presence of both channels in the plasma membrane. Expression of the TASK channels in COS-7 cells resulted in intensive fluorescence also in intracellular membranes, presumably because of the extremely high rate of synthesis as observed with other plasma membrane proteins such as G protein-coupled receptors (not shown).

DISCUSSION

Potassium channels represent by far the largest group of ion channels. In addition to the large number of K^+ channel genes, it is a general phenomenon in the classical families of potassium channels that they show heteromeric assembly of different principal subunits, which further contributes to their extraordinary diversity. Heteromultimers may have different characteristics from any of their contributing homomers, and sometimes (although not always) the assembly to heteromers is the preferred way over homomer formation. Combinations of GIRK1 and GIRK2 or GIRK3 in the brain (31, 32) or GIRK1 and GIRK4 in the heart (33) not only provides channels with new characteristics but renders the otherwise nonfunctional GIRK1 subunit efficient. In the case of the high conductance calcium- and voltage-activated maxi-K channels encoded by the Slo gene, coexpression of the outwardly rectifying Slack yields channels with new pharmacological characteristics and single channel properties (34). In the family of voltage-dependent K^+ channels, specific subcellular localization of $K_V1.2$-$K_V1.4$ (35) and $K_V1.2$-$K_V1.1$ heteromers (36) have been revealed. Possible heterodimerization of different members of the family of 2P channels has been heavily debated and also addressed experimentally (12, 17).

In the present study we demonstrate for the first time that two different subunits of the 2P family of potassium channels, TASK-1 and TASK-3, constitute functional heterodimers in the *Xenopus* expression system. Identification of such heterodimers was possible because of the strikingly different RR and pH sensitivities of the two participating TASK channels. The TASK-1/TASK-3 heterodimer inherited its features asymmetrically from the two parent subunits. The RR insensitivity of the heterodimer is a logical consequence of the need for the binding site to be present in both subunits consistent with the Hill coefficient of 1 for a homodimeric TASK-3 channel. In

contrast, the intermediate pH sensitivity of the tandem channel is an expression of the more complex contribution from both subunits. Comparison of the distribution of data points in the double inhibitory plots derived from tandem channels and coexpressed individual TASK-1 and TASK-3 subunits suggests that heterodimer formation in the latter case is not a rare event and probably is a favored process.

Xenopus oocytes are a convenient way of studying TASK channels because their background K^+ conductance is negligible. The cellular distribution of TASK-3 and TASK-1 channels expressed in a variety of cells is consistent with their primary function in the plasma membrane and would allow the formation of heterodimers. However, demonstration of the existence of heterodimers of endogenous 2P channels in mammalian cells is a more challenging endeavor that will need additional tools and knowledge to accomplish. There may be additional, as yet unknown 2P channels present in cells (the genome of *Caenorhabditis elegans* contains more than 40 genes encoding 2P K^+ channels), and although RR discriminates well between members of TASK currents, it also inhibits TRAAK, and additional 2P channels may also be affected. RR also affects the intermediate and large conductance Ca^{2+}-activated K^+ channels (37), the nonspecific cation channel vanilloid receptor (38), and other more distantly related ion transport mechanisms (39, 40). The lack of specific inhibitors and/or antibodies against the various forms of TASK channels and their close relatives, together with their low single channel conductance and mean open times (in the range of 1 ms (41)) makes discrimination between TASK channels by high resolution electrophysiological studies extremely difficult.

Despite the difficulties in the detection of TASK channels, evidence is accumulating to support their functional importance. The "standing outward" current, $I_{K(SO)}$, of cerebellar granule neurons was identified as the functional correlate of TASK-1 (2), and inhibition of TASK-1 by M_3 muscarinic receptor stimulation has been proposed to regulate neuronal excitability (42). A high level of expression of TASK-1 was indicated by *in situ* hybridization in spinal cord motoneurons and in the brain stem as well as in several other regions of the brain. The inhibition of the pH-sensitive current of hypoglossal motoneurons by serotonin, norepinephrine, and other neurotransmitters was also suggested to be mediated by the effects of these agonists on TASK-1 (3). The presence of TASK-1 and its regulation by angiotensin II has been described in rat adrenal cortex in the glomerulosa layer producing aldosterone (4), and TASK-1 like channels were detected in the chemosensitive cells of the carotid body (5) and of the small airways (43).

Heterodimer formation is likely to be present in cells expressing both TASK-1 and TASK-3 channels. Although the expression pattern of TASK-1 has been investigated by Northern analysis of human, mouse, and rat tissues (21, 22, 41), there are only limited data available on the tissue expression of TASK-3 channels. Because of its very low expression levels, TASK-3 could not be detected in any tissues by Northern blot analysis (24, 25). Recent studies using *in situ* hybridization demonstrated that TASK-3 is expressed in the granule neurons of the developing mouse cerebellum, but its expression declined simultaneously with the appearance of TASK-1 (44). The functional relevance of the simultaneous expression of TASK-1 and TASK-3 in a certain stage of development of cerebellar granule cells (29) is yet to be determined. Interestingly, TASK-3 expression could be easily detected even by Northern analysis in the zona glomerulosa of the rat adrenal cortex tissue.[2] TASK-1 is also expressed in adrenal glomerulosa cells (4), but the high RR and low pH sensitivity of the glomerulosa background K^+ current (4, 30) suggests that the expression of TASK-3 dominates in this tissue and the current of TASK-1/TASK-3 heterodimers (although possibly present) are not responsible for a major conductance in glomerulosa cells.

In summary, the present results demonstrate that certain members of the families of 2P potassium channels, namely TASK-1 and TASK-3 but not TASK-1 and TRAAK, can form functional heterodimers. These heterodimers display regulatory features that are distinct from their parent subunits and may add to the functional diversity of the potassium channel proteins. Further studies will tell whether such heterodimers are formed within the cells of native tissues and reveal their functional significance in regulating excitability and ionic composition.

Acknowledgments—We thank Tamás Balla for access to imaging equipment, support, and valuable discussions. We are grateful to Prof. Michel Lazdunski and Florian Lesage for the pEXO, pEXO-TASK-1, pEXO-TRAAK, and pEXO-TREK-1 plasmids and to K. E. Bernstein for the angiotensin II (AT_{1a}) receptor plasmid construct. We thank Erika Kovács and Irén Veres for skillful technical assistance. The valuable comments of Prof. László Gráf are highly appreciated.

REFERENCES

1. Chavez, R. A., Gray, A. T., Zhao, B. B., Kindler, C. H., Mazurek, M. J., Mehta, Y., Forsayeth, J. R., and Yost, C. S. (1999) *J. Biol. Chem.* **274,** 7887–7892
2. Millar, J. A., Barratt, L., Southan, A. P., Page, K. M., Fyffe, R. E., Robertson, B., and Mathie, A. (2000) *Proc. Natl. Acad. Sci. U. S. A.* **97,** 3614–3618
3. Talley, E. M., Lei, Q., Sirois, J. E., and Bayliss, D. A. (2000) *Neuron* **25,** 399–410
4. Czirják, G., Fischer, T., Spät, A., Lesage, F., and Enyedi, P. (2000) *Mol. Endocrinol.* **14,** 863–874
5. Buckler, K. J., Williams, B. A., and Honore, E. (2000) *J. Physiol.* **525,** 135–142
6. Patel, A. J., and Honore, E. (2001) *Trends Neurosci.* **24,** 339–346
7. Lesage, F., and Lazdunski, M. (2000) *Am. J. Physiol.* **279,** F793–F801
8. Lesage, F., Lauritzen, I., Duprat, F., Reyes, R., Fink, M., Heurteaux, C., and Lazdunski, M. (1997) *FEBS Lett.* **402,** 28–32
9. Lesage, F., Reyes, R., Fink, M., Duprat, F., Guillemare, E., and Lazdunski, M. (1996) *EMBO J.* **15,** 6400–6407
10. Lopes, C. M., Zilberberg, N., and Goldstein, S. A. (2001) *J. Biol. Chem.* **276,** 24449–24452
11. Lesage, F., Guillemare, E., Fink, M., Duprat, F., Lazdunski, M., Romey, G., and Barhanin, J. (1996) *EMBO J.* **15,** 1004–1011
12. Salinas, M., Reyes, R., Lesage, F., Fosset, M., Heurteaux, C., Romey, G., and Lazdunski, M. (1999) *J. Biol. Chem.* **274,** 11751–11760
13. Fink, M., Duprat, F., Lesage, F., Reyes, R., Romey, G., Heurteaux, C., and Lazdunski, M. (1996) *EMBO J.* **15,** 6854–6862
14. Bang, H., Kim, Y., and Kim, D. (2000) *J. Biol. Chem.* **275,** 17412–17419
15. Lesage, F., Terrenoire, C., Romey, G., and Lazdunski, M. (2000) *J. Biol. Chem.* **275,** 28398–28405
16. Fink, M., Lesage, F., Duprat, F., Heurteaux, C., Reyes, R., Fosset, M., and Lazdunski, M. (1998) *EMBO J.* **17,** 3297–3308
17. Rajan, S., Wischmeyer, E., Karschin, C., Preisig-Muller, R., Grzeschik, K. H., Daut, J., Karschin, A., and Derst, C. (2001) *J. Biol. Chem.* **276,** 7302–7311
18. Reyes, R., Duprat, F., Lesage, F., Fink, M., Salinas, M., Farman, N., and Lazdunski, M. (1998) *J. Biol. Chem.* **273,** 30863–30869
19. Girard, C., Duprat, F., Terrenoire, C., Tinel, N., Fosset, M., Romey, G., Lazdunski, M., and Lesage, F. (2001) *Biochem. Biophys. Res. Commun.* **282,** 249–256
20. Decher, N., Maier, M., Dittrich, W., Gassenhuber, J., Bruggemann, A., Busch, A. E., and Steinmeyer, K. (2001) *FEBS Lett.* **492,** 84–89
21. Duprat, F., Lesage, F., Fink, M., Reyes, R., Heurteaux, C., and Lazdunski, M. (1997) *EMBO J.* **16,** 5464–5471
22. Leonoudakis, D., Gray, A. T., Winegar, B. D., Kindler, C. H., Harada, M., Taylor, D. M. C.-R., Forsayeth, J. R., and Yost, C. S. (1998) *J. Neurosci.* **18,** 868–877
23. Lopes, C. M., Gallagher, P. G., Buck, M. E., Butler, M. H., and Goldstein, S. A. (2000) *J. Biol. Chem.* **275,** 16969–16978
24. Kim, Y., Bang, H., and Kim, D. (2000) *J. Biol. Chem.* **275,** 9340–9347
25. Rajan, S., Wischmeyer, E., Liu, G. X., Müller, R. P., Daut, J., Karschin, A., and Derst, C. (2000) *J. Biol. Chem.* **275,** 16650–16657
26. Czirják, G., Petheō, G. L., Spät, A., and Enyedi, P. (2001) *Am. J. Physiol.* **281,** C700–C708
27. Goldstein, S. A., Bockenhauer, D., O'Kelly, I., and Zilberberg, N. (2001) *Nat. Rev. Neurosci.* **2,** 175–184
28. Maingret, F., Fosset, M., Lesage, F., Lazdunski, M., and Honore, E. (1999) *J. Biol. Chem.* **274,** 1381–1387
29. Medhurst, A. D., Rennie, G., Chapman, C. G., Meadows, H., Duckworth, M. D., Kelsell, R. E., Gloger, I. I., and Pangalos, M. N. (2001) *Brain Res. Mol. Brain Res.* **86,** 101–114
30. Szabadkai, G., Várnai, P., and Enyedi, P. (1999) *Biochem. Pharmacol.* **57,** 209–218
31. Lesage, F., Guillemare, E., Fink, M., Duprat, F., Heurteaux, C., Fosset, M., Romey, G., Barhanin, J., and Lazdunski, M. (1995) *J. Biol. Chem.* **270,** 28660–28667

32. Kofuji, P., Davidson, N., and Lester, H. A. (1995) *Proc. Natl. Acad. Sci. U. S. A.* **92,** 6542–6546
33. Krapivinsky, G., Gordon, E. A., Wickman, K., Velimirovic, B., Krapivinsky, L., and Clapham, D. E. (1995) *Nature* **374,** 135–141
34. Joiner, W. J., Tang, M. D., Wang, L. Y., Dworetzky, S. I., Boissard, C. G., Gan, L., Gribkoff, V. K., and Kaczmarek, L. K. (1998) *Nat. Neurosci.* **1,** 462–469
35. Sheng, M., Liao, Y. J., Jan, Y. N., and Jan, L. Y. (1993) *Nature* **365,** 72–75
36. Wang, H., Kunkel, D. D., Martin, T. M., Schwartzkroin, P. A., and Tempel, B. L. (1993) *Nature* **365,** 75–79
37. Wu, S. N., Jan, C. R., and Li, H. F. (1999) *J. Pharmacol. Exp. Ther.* **290,** 998–1005
38. Dray, A., Forbes, C. A., and Burgess, G. M. (1990) *Neurosci. Lett.* **110,** 52–59
39. Cibulsky, S. M., and Sather, W. A. (1999) *J. Pharmacol. Exp. Ther.* **289,** 1447–1453
40. Hirano, M., Imaizumi, Y., Muraki, K., Yamada, A., and Watanabe, M. (1998) *Pfluegers Arch. Eur. J. Physiol.* **435,** 645–653
41. Kim, Y., Bang, H., and Kim, D. (1999) *Am. J. Physiol.* **277,** H1669–H1678
42. Boyd, D. F., Millar, J. A., Watkins, C. S., and Mathie, A. (2000) *J. Physiol.* **529,** 321–331
43. O'Kelly, I., Stephens, R. H., Peers, C., and Kemp, P. J. (1999) *Am. J. Physiol.* **276,** L96–L104
44. Brickley, S. G., Revilla, V., Cull-Candy, S. G., Wisden, W., and Farrant, M. (2001) *Nature* **409,** 88–92